Int. J. Electrochem. Sci., 15 **(2020)** 8506 – 8511, doi: 10.20964/2020.09.08

International Journal of
ELECTROCHEMICAL
SCIENCE
www.electrochemsci.org

Short Communication

Structure Characterization and Electrical Properties of $Sn_{0.9}Ga_{0.1}P_2O_7/KH_2PO_4/KPO_3$ Composite Electrolyte for Medium Temperature Fuel Cells

Yan Han[**], *Zikun Rong, Tianhui Hu, Peng Sun, Lin Sun*[*], *Hui Miao*[*]

Anhui Provincial Key Laboratory for Degradation and Monitoring of Pollution of the Environment; School of Chemical and Material Engineering, Fuyang Normal University, Fuyang 236037, China
[*]E-mail: hanyan624000@126.com, 200807011@fynu.edu.cn, 200107025@fynu.edu.cn

Received: 5 May 2020 / *Accepted:* 1 July 2020 / *Published:* 10 August 2020

In this study, $Sn_{0.9}Ga_{0.1}P_2O_7/KH_2PO_4/KPO_3$ was synthesized by solid-phase method. The sample was characterized by Raman spectrometer and X-ray diffractometer. The ionic conductivity of $Sn_{0.9}Ga_{0.1}P_2O_7/KH_2PO_4/KPO_3$ at 400–700 °C was studied by electrochemical methods, including impedance spectroscopy, oxygen concentration discharge cell and hydrogen/oxygen fuel cell. The oxygen concentration discharge cell result showed that the sample is a pure oxygen ion conductor in an oxidizing atmosphere. The maximum current and power output density of $Sn_{0.9}Ga_{0.1}P_2O_7/KH_2PO_4/KPO_3$ are 380 $mA \cdot cm^{-2}$ and 134 $mW \cdot cm^{-2}$ at 700 °C, respectively.

Keywords: X-ray diffraction; Conductivity; Electrolyte; Fuel cell; Composite

1. INTRODUCTION

Solid oxide fuel cells (SOFCs) have become research hotspots because of theirs unique all-solid structure, wide range of fuel use, etc [1–5]. In general, the operation temperatures of traditional SOFCs are too high (700–900 °C), requiring high performance of the electrolyte, electrode and other materials. Therefore, development of medium and low temperature SOFCs has become an inevitable trend [6–10].

Due to the high protonic conductivities in the temperature range of 100–400 °C, SnP_2O_7 based electrolytes are highly valued [11–14]. Ma et al. found that $Sn_{0.94}Sc_{0.06}P_2O_7$ had the highest conductivity of, 2.8×10^{-2} $S \cdot cm^{-1}$, in wet hydrogen at 200 °C. However, the reduction of Sn^{4+} reduced the mechanical property and conductivity above 200 °C [14]. In order to improve the performance of the electrolyte, a composite electrolyte was proposed [15–18]. Hibino et al. synthesized a new

inorganic-organic composite of $Sn_{0.95}Al_{0.05}P_2O_7$/polystyrene- b-poly(ethylene/propylene)-b-polystyrene [18].

In order to inhibit the reduction of Sn^{4+} and extend the application temperature range, this paper synthesizes composite electrolyte by reacting K_2CO_3 salt with Ga^{3+}-doped SnP_2O_7. Structure characterization and medium temperature electrical properties of $Sn_{0.9}Ga_{0.1}P_2O_7/KH_2PO_4/KPO_3$ are also investigated.

2. EXPERIMENTAL

According to the molecular formula, Ga_2O_3, SnO_2, K_2CO_3 and 85 % H_3PO_4 were weighed. The reactants were heated with an alcohol lamp with continuous stirring and evaporating to obtain a light gray block. After grinding, the powder was calcined at 500 °C for 2 h. A $Sn_{0.9}Ga_{0.1}P_2O_7/KH_2PO_4/KPO_3$ sheet (thickness: 1.2 mm) was prepared by dry pressing at 200 MPa and it was sintered at 700 °C for 1 h.

The crystal structure of the sample was determined by Raman spectrometer and X-ray diffractometer. The AC impedance of $Sn_{0.9}Ga_{0.1}P_2O_7/KH_2PO_4/KPO_3$ in air was measured with CHI660E measuring instrument (frequency range: 1 Hz-100 kHz) at 400–700 °C and converted into conductivity. The oxygen concentration discharge cell represented by the cell (1) and the hydrogen/oxygen fuel cell indicated by the cell (2) were measured, respectively.

air, Pd-Ag|$Sn_{0.9}Ga_{0.1}P_2O_7/KH_2PO_4/KPO_3$|Pd-Ag, O_2 cell (1)

H_2, Pd-Ag|$Sn_{0.9}Ga_{0.1}P_2O_7/KH_2PO_4/KPO_3$|Pd-Ag, O_2 cell (2)

3. RESULTS AND DISCUSSION

Fig. 1 shows the Raman spectrum of $Sn_{0.9}Ga_{0.1}P_2O_7/KH_2PO_4/KPO_3$. The characteristic peaks at 352 cm^{-1} and 520 cm^{-1} are the bending vibration of PO_4 tetrahedron and P-O-P structural unit in phosphate, respectively. The band near 620 cm^{-1} belongs to the symmetric stretching vibration of P-O-P in metaphosphate. The vibrations at 749 cm^{-1} and 1097 cm^{-1} belong to the symmetric stretching vibration of bridged oxygen group P-O-P and non-bridged oxygen group in pyrophosphate, correspondingly [19]. The vibration peak at 925 cm^{-1} belongs to the symmetric stretching vibration of non-bridged oxygen group in phosphate. The band near 1165 cm^{-1} belongs to the symmetric stretching vibration of non-bridged oxygen group in metaphosphate. The results show that the structure of the sample is mainly composed of pyrophosphate group and a small amount of phosphate and metaphosphate group.

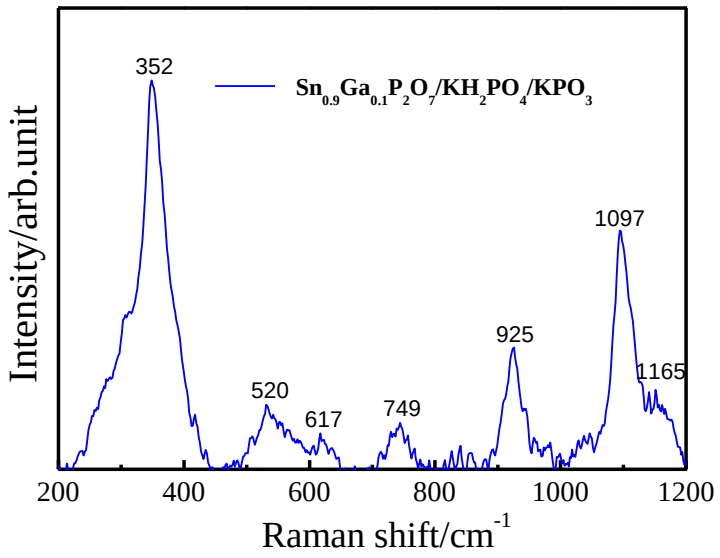

Figure 1. Raman spectrum of $Sn_{0.9}Ga_{0.1}P_2O_7/KH_2PO_4/KPO_3$.

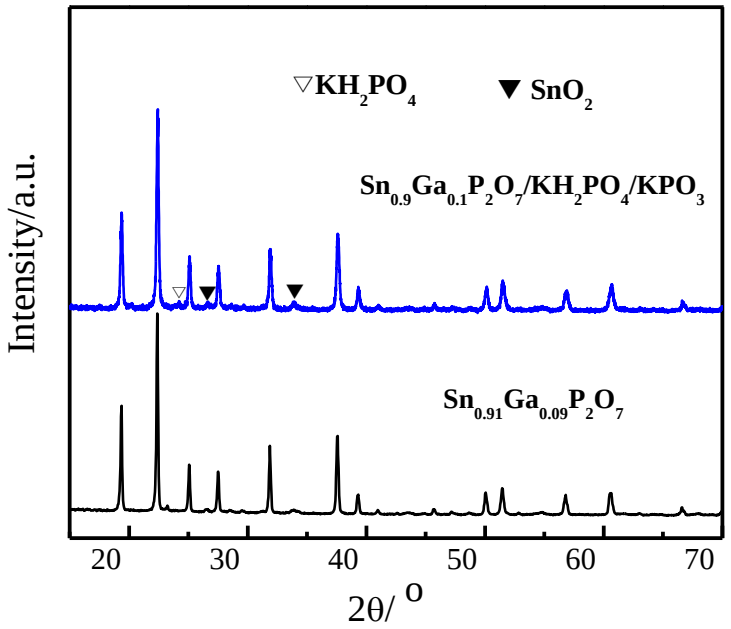

Figure 2. XRD pattern of $Sn_{0.9}Ga_{0.1}P_2O_7/KH_2PO_4/KPO_3$.

Fig. 2 is the XRD spectrum of $Sn_{0.9}Ga_{0.1}P_2O_7/KH_2PO_4/KPO_3$. Comparing it with the XRD spectrum of $Sn_{0.91}Ga_{0.09}P_2O_7$, it can be seen that the diffraction peak positions and intensities are basically the same [13]. In addition, the existence of SnO_2 and KH_2PO_4 second phase are also found. This may be due to H_3PO_4 and SnP_2O_7 reacting with K_2CO_3 during the synthesis process: $SnP_2O_7 + K_2CO_3 = SnO_2 + 2KPO_3 + CO_2\uparrow$ and $2H_3PO_4 + K_2CO_3 = H_2O + CO_2\uparrow + 2KH_2PO_4$. At the same time, most of the potassium salts are amorphous.

The Arrhenius curve of $Sn_{0.9}Ga_{0.1}P_2O_7/KH_2PO_4/KPO_3$ in air is shown in Fig. 3 and it compared with the conductivities of the samples reported in the literatures [13, 20]. It can be seen that the

conductivities of $Sn_{0.9}Ga_{0.1}P_2O_7/KH_2PO_4/KPO_3$ composite electrolyte are significantly enhanced compared with the single-doped sample. The conductivity reaches 1.8×10^{-2} S·cm^{-1} at 700 °C. The conductivity of $Sn_{0.9}Ga_{0.1}P_2O_7/KH_2PO_4/KPO_3$ is several orders of magnitude higher than that reported by S.R. Phadke et al. [20]. This may be due to the fact that the proton transport ability in the composite electrolyte is greatly enhanced. There is a big gap between the results of Phadke et al. [20] and Wang et al. [13]. This may be mainly due to the differences in the preparation process of the materials and high temperature volatilization.

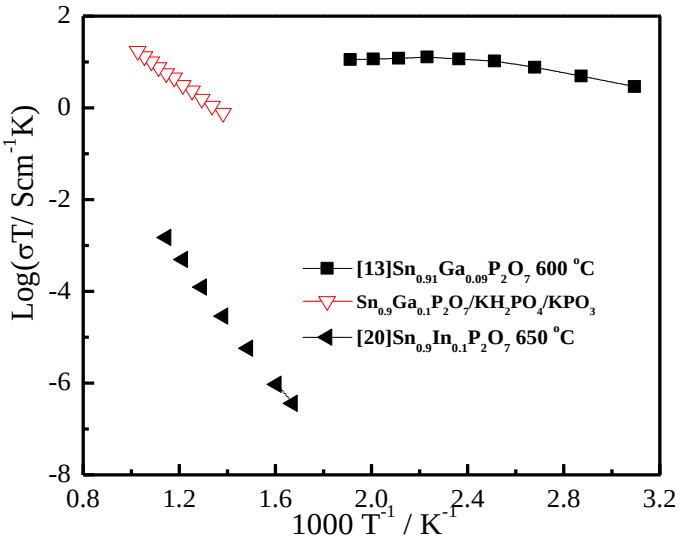

Figure 3. The Arrhenius curves of $Sn_{0.9}Ga_{0.1}P_2O_7/KH_2PO_4/KPO_3$, $Sn_{0.91}Ga_{0.09}P_2O_7$ and $Sn_{0.9}In_{0.1}P_2O_7$.

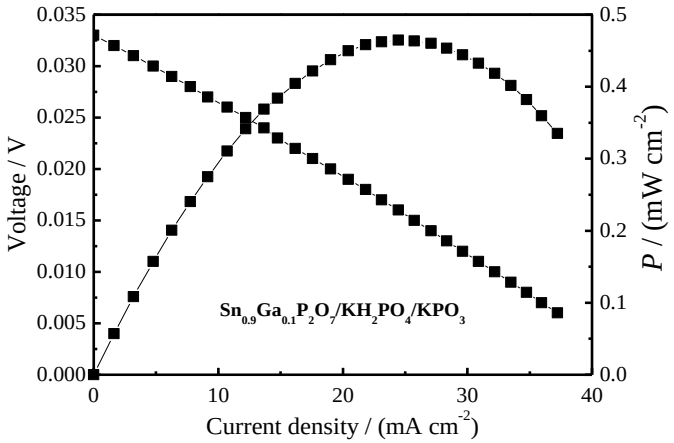

Figure 4. Oxygen concentration discharge cell: air, Pd-Ag|$Sn_{0.9}Ga_{0.1}P_2O_7/KH_2PO_4/KPO_3$|Pd-Ag, O_2 at 700 °C.

The oxide ionic conduction of $Sn_{0.9}Ga_{0.1}P_2O_7/KH_2PO_4/KPO_3$ in an oxygen atmosphere was determined by oxygen concentration discharge cell, as shown in Fig.4. The theoretical electromotive force value of oxygen concentration discharge cell is calculated according to the Nernst equation when

the sample is a pure oxygen ion conductor. It can be seen from Fig.4 that the measured open circuit voltage of oxygen concentration discharge cell is in good agreement with the theoretical value. It is shown that the sample is a pure ionic conductor under an oxidizing atmosphere at 700 °C.

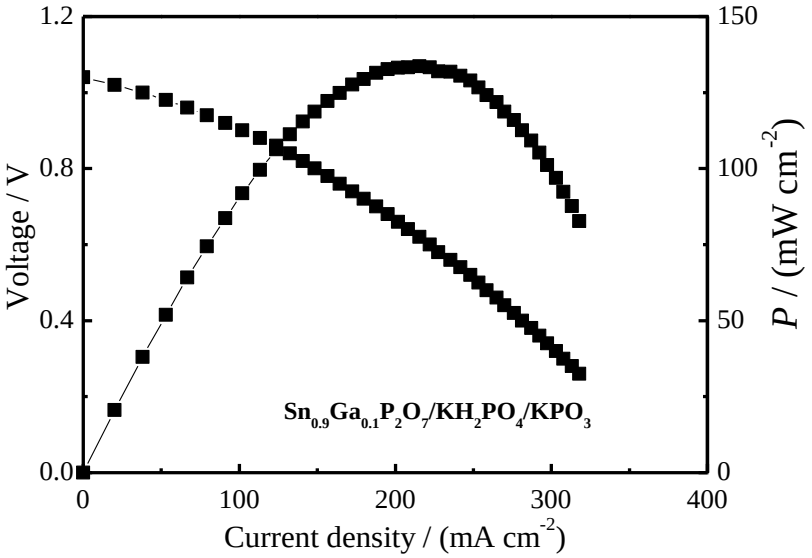

Figure 5. *I-V-P* curves of $Sn_{0.9}Ga_{0.1}P_2O_7/KH_2PO_4/KPO_3$ at 700 °C.

The current-voltage-power (*I-V-P*) curves using $Sn_{0.9}Ga_{0.1}P_2O_7/KH_2PO_4/KPO_3$ as electrolyte were tested. The results are shown in Fig. 5. The open circuit voltage is 1.04 V at 700 °C. The theoretical electromotive force of the hydrogen/oxygen fuel cell at the corresponding temperature is 1.12 V. Therefore, the ion migration number is 0.93. It can be seen that there is a certain degree of electrons in the sample under the hydrogen/oxygen fuel cell condition. This may be due to the reduction of Sn^{4+} to Sn^{2+}. The maximum current and power output density of $Sn_{0.9}Ga_{0.1}P_2O_7/KH_2PO_4/KPO_3$ are 380 mA·cm^{-2} and 134 mW·cm^{-2} at 700 °C, respectively.

4. CONCLUSIONS

In this study, $Sn_{0.9}Ga_{0.1}P_2O_7/KH_2PO_4/KPO_3$ was synthesized by solid-phase method. The Raman spectrum and XRD results showed that the sample structure is mainly composed of pyrophosphate group and a small amount of phosphate and metaphosphate group. The conductivity reaches 1.8×10^{-2} S·cm^{-1} at 700 °C. The maximum current and power output density of $Sn_{0.9}Ga_{0.1}P_2O_7/KH_2PO_4/KPO_3$ are 380 mA·cm^{-2} and 134 mW·cm^{-2} at 700 °C, respectively.

ACKNOWLEDGEMENTS
This work was supported by the horizontal cooperation project of Fuyang municipal government and Fuyang Normal University (XDHX2016019, XDHXTD201704), the horizontal cooperation project of Fuyang Normal University (HX2020016).

CONFLICTS OF INTEREST
The authors declare no conflicts of interest.

References

1. L. Bi, S.P. Shafi, E.H. Da'as and E. Traversa, *Small*, 14 (2018) 1801231.
2. C. Bernuy-Lopez, L. Rioja-Monllor, T. Nakamura, S. Ricote, R. O'Hayre, K. Amezawa, M. Einarsrud and T. Grande, *Materials*, 11 (2018) 196.
3. 3.Y.P. Xia, Z.Z. Jin, H.Q. Wang, Z.Gong, H.L. Lv, R.R. Peng, W. Liu and L. Bi, *J. Mater. Chem. A*, 7 (2019) 16136.
4. Y. Tian, Z. Lü, X. Guo and P. Wu, *Int. J. Electrochem. Sci*., 14 (2019) 1093.
5. X. Xu, L. Bi and X.S. Zhao, *J. Membrane Sci.*, 558 (2018) 17.
6. A.A. Solovyev, S.V. Rabotkin, A.V. Shipilova and I.V. Ionov, *Int. J. Electrochem. Sci*., 14 (2019) 575.
7. X. Xu, H.Q. Wang, J.M. Ma, W.Y. Liu, X.F. Wang, M. Fronzi and L. Bi, *J. Mater. Chem. A*, 7 (2019) 18792.
8. H. Jiang and F. Zhang, *Int. J. Electrochem. Sci*., 15 (2020) 959.
9. J.M. Ma, Z.T. Tao, H.N. Kou, M. Fronzi and L. Bi, *Ceram. Int.*, 46 (2020) 4000.
10. H. Dai, H. Kou, Z. Tao, K. Liu, M. Xue, Q. Zhang, L. Bi, *Ceram. Int.*, 46 (2020) 6987.
11. M. Nagao, T. Kamiya, P. Heo, A. Tomita, T. Hibino and M. Sano, *J. Electrochem. Soc.*, 153 (2006) A1604.
12. A. Tomita, N. Kajiyama, T. Kamiya, M. Nagao and T. Hibino, *J. Electrochem. Soc.*, 154 (2007) B1265.
13. H. Wang, J. Liu, W. Wang and G. Ma, *J. Power Sources*, 195 (2010) 5596.
14. H. Wang, H. Zhang, G. Xiao, F. Zhang, T. Yu, J. Xiao and G. Ma, *J. Power Sources*, 196 (2011) 683.
15. Y.C. Jin, M. Nishida, W. Kanematsu and T. Hibino, *J. Power Sources*, 196 (2011) 6042.
16. Y. Sato, Y.B. Shen, M. Nishida, W. Kanematsu and T. Hibino, *J. Meter. Chem.*, 22 (2012) 3973.
17. B. Singh, A. Bhardwaj, S. K. Gautam, D. Kumar, O. Parkash, I.-H. Kim and S.-J. Song, *J. Power Sources*, 345 (2017) 176.
18. Y. Jin and T. Hibino, *Electrochim. Acta*, 55 (2010) 8371.
19. P. A. Bingham and R. J. Hand, *Mater. Res. Bull.*, 43 (2018) 1679.
20. S.R. Phadke, C.R. Bowers, E.D. Wachsman and J.C. Nino, *Solid State Ionics*, 183 (2011) 26.